Mahmoudi M., et al., *BioImpacts,* 2016, 6(2), 111-115
doi: 10.15171/bi.2016.16
http://bi.tbzmed.ac.ir/

Infection-resistant MRI-visible scaffolds for tissue engineering applications

Morteza Mahmoudi[1,2,3], Mingming Zhao[4], Yuka Matsuura[2], Sophie Laurent[5,6], Phillip C. Yang[1,2], Daniel Bernstein[1,4], Pilar Ruiz-Lozano[1,4*], Vahid Serpooshan[1,4*]

[1]Stanford Cardiovascular Institute, Stanford, CA, 94305 USA
[2]Division of Cardiovascular Medicine, Stanford University, 300 Pasteur Dr., Stanford, CA 94305
[3]Nanotechnology Research Center and Department of Nanotechnology, Faculty of Pharmacy, Tehran University of Medical Sciences, Tehran, 14155-6451, Iran
[4]Department of Pediatrics, Stanford University, 300 Pasteur Dr., Stanford, CA 94305
[5]Department of General, Organic, and Biomedical Chemistry, NMR and Molecular Imaging Laboratory, University of Mons, Avenue Maistriau, 19, B-7000 Mons, Belgium
[6]CMMI - Center for Microscopy and Molecular Imaging, Avenue A. Bolland, 8 B-6041 Gosselies, Belgium

Article Info

Article Type:
Short Communication

Article History:
Received: 07 July 2016
Accepted: 12 July 2016
ePublished: 15 July 2016

Keywords:
Antibacterial properties,
Collagen scaffold,
Magnetic resonance imaging,
SPION,
Superparamagnetic iron oxide nanoparticles,
Tissue engineering

Summary

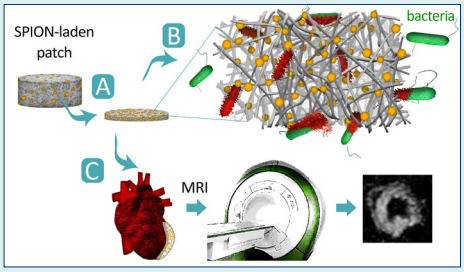

Tissue engineering utilizes porous scaffolds as template to guide the new tissue growth. Clinical application of scaffolding biomaterials is hindered by implant-associated infection and impaired *in vivo* visibility of construct in biomedical imaging modalities. We recently demonstrated the use of a bioengineered type I collagen patch to repair damaged myocardium. By incorporating superparamagnetic iron oxide nanoparticles into this patch, here, we developed an MRI-visible scaffold. Moreover, the embedded nanoparticles impeded the growth of Salmonella bacteria in the patch. Conferring anti-infection and MRI-visible activities to the engineered scaffolds can improve their clinical outcomes and reduce the morbidity/mortality of biomaterial-based regenerative therapies.

Biodegradable scaffold systems are a promising tool for regenerative therapies.[1,2] In addition, scaffold constructs are engineered as biomimetic, three-dimensional (3D) models to recapitulate and study the cellular and molecular biology underlying various diseases *in vitro*.[3,4] However, both *in vitro* and *in vivo* application of tissue engineering scaffolds have been challenged by the difficulty to achieve germ-free biomaterials for safe therapeutic use. Biomaterial-associated biofilm and infection have been increasingly identified as one of the primary failure mechanisms of implanted medical devices (e.g., catheters, stents, and mechanical heart valves), yet these phenomena have not been well investigated in the context of tissue engineering 3D scaffolds.

Another factor limiting the clinical application of tissue engineering grafts is the lack of efficient, noninvasive techniques for *in situ*-tracking of the scaffold (e.g., its location, integration, and degradation) after implantation.[5-8] This would be of significance particularly in the case of internal tissue implants, such as cardiac patches, where the structural and spatial constraints of the tissue structure further hamper monitoring the scaffold function post implantation.

We recently demonstrated the use of a bioengineered

***Corresponding author:** Pilar Ruiz-Lozano, Email: prlozano@stanford.edu; Vahid Serpooshan, Email: vserp1@stanford.edu

cardiac patch, consisting of type I collagen and a cardioprotective (follistatin-like 1) protein, to repair damaged myocardium.[1,9,10] One potential hurdle for extensive clinical application of the developed patch could be biomaterial-associated infection. To address this issue, in this study, a revised, infection-resistant generation of the collagen scaffold system was designed by incorporating anti-microbial superparamagnetic iron oxide nanoparticles (SPIONs[11,12]) into the engineered construct. The embedded, biocompatible, spherical SPIONs also yielded a significant contrast in the magnetic resonance imaging (MRI) of the construct, hence producing an anti-infective, MRI-visible scaffold system.[13] It is noteworthy that we and others showed excellent *in vitro* and *in vivo* biocompatibility of SPIONs with various surface coatings.[14,15]

Collagen gels were fabricated by mixing rat tail type I collagen solution (1.1 ml of 3.84 mg/ml, Millipore, MA, US) with 0.9 ml sterile phosphate buffered saline (PBS) and neutralizing by NaOH as previously described.[3,16] Hydrated gels subsequently underwent plastic compression[4,17] by applying a compressive stress of 1400 N/m^2 for 5 min, yielding a dense biomaterial with increased stiffness (Young modulus) approaching that to the native myocardium[1,4,9,10,16] (Fig. 1A). The iron oxide nanoparticles (diameter of 17.8 ± 2.6 nm with a surface charge of 32.6 ± 0.3 mv) were coated with aminopropyltriethoxysilane (APTES) and added to the liquid collagen solution at different concentrations (1.5, 3, and 6 µg/mL or µg/scaffold) prior to neutralization, followed by gelation and plastic compression. We selected APTES coating mainly because of its excellent protein-attachment capability which facilitates incorporation of SPIONs to the collagen fibers.[18] Detailed information about synthesis and characterization of the APTES nanoparticles is previously described.[18] Scanning electron microscopy of particle-laden scaffolds demonstrated rather uniform distribution and incorporation of the SPIONs within the collagen fibrils (Fig. 1B).

The effect of SPIONs incorporation on the MRI-visibility of engineered collagen scaffolds was tested both *in vitro* and *in vivo* (Fig. 2). *In vitro*, T2* weighted images demonstrated a remarkable contrast induced by magnetic nanoparticles seeded in the gels, particularly at 3 and 6 µg/mL, in comparison to the control (empty) scaffolds (Fig. 2B). For the *in vivo* imaging, collagen scaffolds were grafted onto the epicardial surface of the heart in male, 12 weeks old C57BL/6J mice (Jackson Laboratories, Bar Harbor, ME, USA) via left thoracotomy.[1,10] All procedures involving animal use, housing, and surgeries were approved by the Stanford Institutional Animal Care and Use Committee (IACUC). The animal groups included: 1) empty (control) patch, 2) SPION-laden patch, and 3) a sandwich structure consisting of empty and particle-loaded patches (Fig. 2C, *n=2*). Manganese Enhanced MRI (MEMRI) imaging, conducted 2 h following the implantation, demonstrated a significant contrast in SPION-laden scaffolds (groups 2 and 3). Arrows in Fig. 2C point to the location of the SPION-laden patches on the myocardium.

SPIONs have been recently used for the treatment of a variety of antibiotic-resistant biofilms (e.g., gentamicin-resistant staphylococci) in monolayer culture conditions.[19-21] Whether addition of SPIONs to 3D culture systems confers them antibacterial activity has not been investigated. Nanoparticles can disrupt bacterial membrane and enter into their intracellular environment.[22] Membrane disruption and release of toxic ions are considered as the main mechanisms of anti-bacterial effect of nanoparticles.[22] SPIONs have shown significant anti-bacterial effect on different types of bacteria; here, we used Salmonella as model bacteria[19,23].

We tested the bacteria-resistivity of SPION-laden 3D collagen scaffolds by growing Salmonella bacteria in the

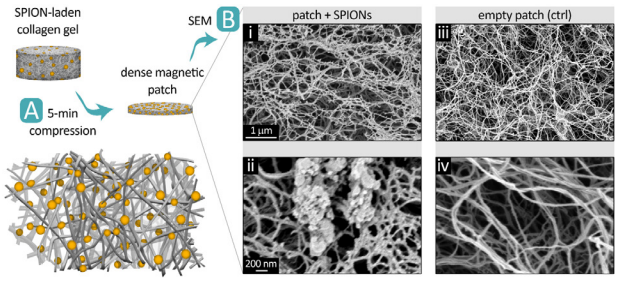

Fig. 1. Schematic illustration of preparation of the patches laden with superparamagnetic iron oxide nanoparticles (SPIONs); **A**: Plastic compression of hydrated collagen gels[10,24]– with or without nanoparticles – produced dense magnetic scaffolds (patches). **B**: scanning electron microscopy of the SPIONs-loaded patch (**i** and **ii**) and empty patch (**iii** and **iv**, control) ultrastructure.

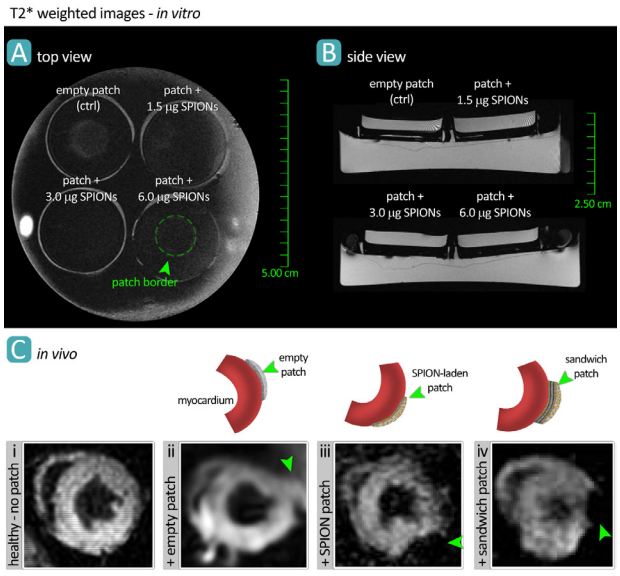

Fig. 2. Magnetic resonance imaging (MRI) of empty (negative control) and SPION-loaded collagen patches at 1.5, 3.0, and 6.0 µg/scaffold concentrations. T1 weighted image from top (**A**) and T2* weighted image from side (**B**) views demonstrated the resulting remarkable contrast in the magnetic patches. The dashed green line and arrow highlight the boundary of the patch. **C**: *In vivo* manganese-enhanced MRI imaging of healthy mouse heart with no treatment (**i**), or grafted with empty patch (**ii**), SPION-loaded patch (**iii**), and loaded-empty-loaded sandwich patch (**iv**). Schemes and arrows show the location and structure of the patch construct grafted onto the myocardium.

scaffolds containing varying quantities of particles (4 to 16 µg/scaffold, *n*=3, the data for highest particle concentration is shown here). Remarkably, collagen scaffolds with or without SPIONs demonstrated a favorable microenvironment for the bacterial growth at 24 and 48 h post infection, when compared with those grown in PBS or the inoculum (controls) (*n*=3, Fig. 3A). This can be attributed to the highly porous ultrastructure of the scaffold which provides ample surface area for the bacteria to anchor. The presence of SPIONs within the collagen matrix yielded no significant effect on the Salmonella growth when compared to that in the empty scaffolds. This could be due to the insufficient dose of particles in the patch, or the fact that the particles added prior to collagen polymerization could be potentially captured within the fibrillar structure, hence, reducing their capability to penetrate into the bacteria. The latter hypothesis was confirmed by scanning electron microscopy (Fig. 1). Addition of 10% antibiotics (v/v, penicillin-streptomycin) to the culture fully demolished the infections. Consistent with previous reports, direct administration of SPIONs to the bacteria culture partially inhibited their growth (Fig. 3A,B).

SPIONs titration assay (Fig. 3B) demonstrated that particle concentrations greater than 32 µg/mL could effectively inhibit the Salmonella growth in the PBS environment. However, this value exceeded the maximum particle concentration that could still allow collagen gelation (16 µg/mL). To load the collagen scaffolds with greater quantities of unbound SPIONs (not captured within nano-fibrillar

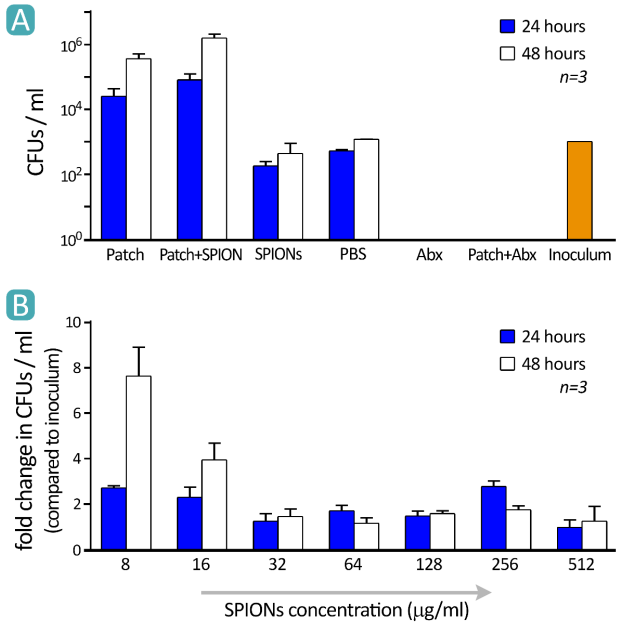

Fig. 3. Antibacterial effect of superparamagnetic iron oxide nanoparticles (SPIONs) embedded in collagen patch. **A**: Salmonella growth in various environments including empty patch, patch loaded with SPIONs (16 µg/ml or /patch), SPIONs alone (16 µg/mL in PBS), pure PBS, PBS + 1% antibiotics (Abx: *penicillin-streptomycin*), patch in PBS + 1% Abx, and the inoculum. Growth data (CFUs/ml) are reported after 24 and 48 h of incubation. **B**: Fold change in Salmonella growth (compared to inoculum) in PBS containing varying levels of SPIONs, ranging from 8 to 512 µg/mL.

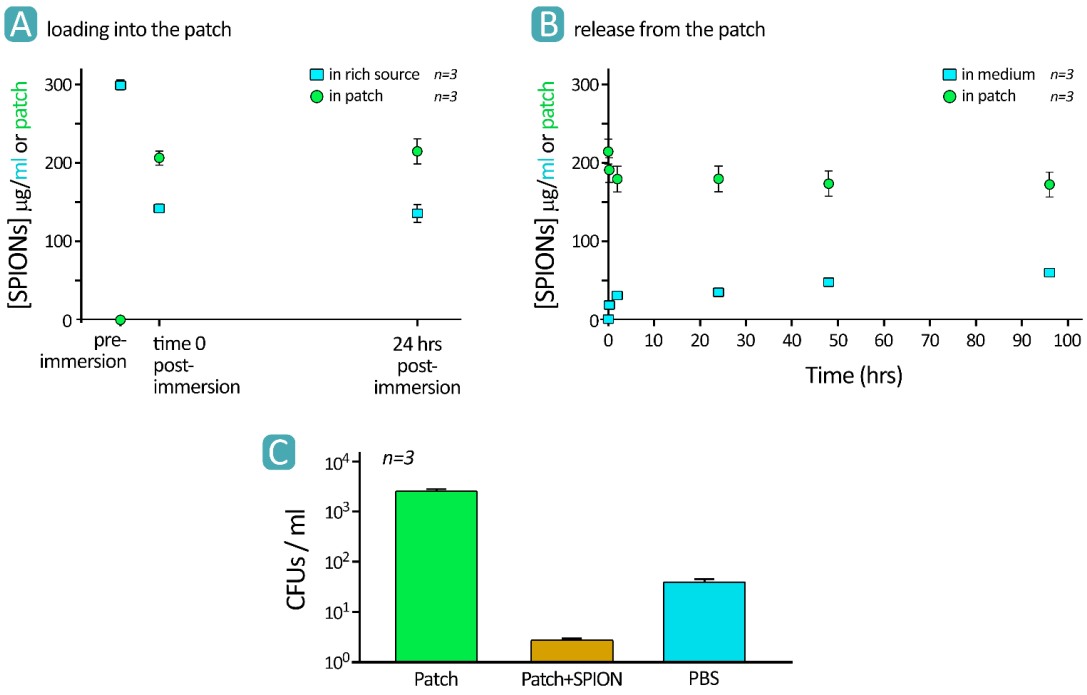

Fig. 4. Loading collagen scaffolds (patches) with SPIONs by direct immersion of the patch in a rich source of particles; **A**: loading phase; Atomic absorption of the supernatants show a decrease in [SPIONs] in the rich source (blue, from ~300 to ~135 µg/ml), associated with an increase in [SPIONs] in the patch (green, from 0 to 214 µg/scaffold). **B**: release test; release of SPION-loaded patches into fresh, empty PBS medium showed a decrease followed by a plateau in [SPIONs] in patch (green) after 4 days of incubation on a shaking plate. This was accompanied by an increase of [SPIONs] in PBS (blue). **C**: Salmonella growth test in the patch loaded with SPIONs, in comparison to the empty patch and PBS.

collagen matrix), polymerized and compressed scaffolds were immersed in a rich source of nanoparticles (300 µg/mL) for the duration of 24 h (Fig. 4A). This resulted in loading particles at a concentration of 214 ± 46 µg/ mL or scaffold as measured by atomic absorption (from supernatants). While the former approach (adding SPIONs during gelation) resulted in entrapment of particles within the 3D fibrillar structure of scaffold, the latter (immersion) method loaded the particles into the porous construct via a diffusion process driven by the concentration gradient of SPIONs.

The particle release from loaded scaffolds was assessed by immersing them in fresh PBS environment and measuring the iron oxide concentration in the supernatant via atomic absorption in a timely fashion (Fig. 4B). SPIONs concentration in the patch reached a plateau after 2 h of incubation in PBS, suggesting that the remaining SPIONs were stable within the scaffold construct for longer terms. Therefore, following 2-hour incubation in PBS, loaded scaffolds were used for the bacteria growth study (Fig. 4C). Remarkably, the SPION-laden scaffolds demonstrated a significant effect ($p < 0.05$) in reducing the bacterial growth (relative to inoculum) when compared to those grown in PBS. Consistent with previous set of data (Fig. 3), the empty scaffolds yielded the highest level of Salmonella growth among all groups. Since SPION concentrations equal or greater than 6 µg/patch were sufficient to yield distinguishable contrast in T2* weighted MRI images (up to 300 µg/patch was tested), the collagen patches loaded with 200µg/patch SPIONs can provide an optimal scaffold system with both MRI-visibility and anti-infective properties.

In summary, here we introduce a new generation of tissue engineering scaffold systems, laden with superparamagnetic iron oxide nanoparticles that are MRI-visible both *in vitro* and *in vivo*. While the typical (empty) collagen gel scaffolds demonstrated to be radically cultivating environment for bacterial growth, the embedded nanoparticles in these scaffolds significantly impeded the scaffold infection. Incorporating anti-infection and MRI-visible properties into regenerative medicine therapies could improve clinical outcomes and reduce the morbidity and mortality associated with biomaterial implant-associated infections. Investigating the fate/biodegradation of the SPION-loaded patch *in vivo*, the effect on inflammatory markers and oxidative stress, and potential effect of particles on the inherent function of the engineered patch are some of the future research directions.

Ethical approval

There is none to be disclosed.

Competing interests

Authors declare no competing interests.

Acknowledgments

This work was supported by National Institutes of Health grants HL65484 and HL086879 (to PRL) and 1K99HL127295 (to VS). VS was an Oak Foundation postdoctoral fellow at Stanford. DB was supported by NIG grant HL061535. SL thanks the Fonds National pour la Recherche Scientifique (F.R.S.-FNRS), the FEDER, the Walloon Region, the COST Actions, the Centre for Microscopy and Molecular Imaging (CMMI) supported by the European Regional Development Fund of the Walloon region, the ARC and UIAP programs. We would like to thank Drs. Marta Andrés Terré, Nicholas A. Eisele, and Denise M. Monack (Dept. of Microbiology and Immunology, Stanford University) for the help with the bacteria work.

Study Highlights

What is current knowledge?

√ The application of superparamagnetic nanoparticles in regenerative medicine has advanced rapidly, offering great promise to develop novel technologies for the diagnosis and therapy of various diseases, in particular, cardiovascular disorders.

√ Engineered 3D tissue constructs, however, are primarily associated with poor *in vivo* traceability which in turn limits their clinical applications.

√ The risk of biomaterial-associated infections has been always a limiting factor.

What is new here?

√ By incorporating superparamagnetic iron oxide nanoparticles into 3D collagen scaffolds, it was found that a new generation of tissue engineering scaffolds with unique antimicrobial and MRI-visible properties can be developed.

√ This technology provides a versatile platform for generating a large number of bioengineered complex 3D tissues for clinical and translational applications.

References

1. Serpooshan V, Zhao M, Metzler SA, Wei K, Shah PB, Wang A, et al. The effect of bioengineered acellular collagen patch on cardiac remodeling and ventricular function post myocardial infarction. *Biomaterials* **2013**; 34: 9048-55. doi:10.1016/j.biomaterials.2013.08.017.
2. Karfeld-Sulzer LS, Waters EA, Kohlmeir EK, Kissler H, Zhang X, Kaufman DB, et al. Protein polymer MRI contrast agents: Longitudinal analysis of biomaterials in vivo. *Biomed Eng Comput Biol* 2014; **6**: 13–20.
3. Serpooshan V, Quinn TM, Muja N, Nazhat SN. Hydraulic permeability of multilayered collagen gel scaffolds under plastic compression-induced unidirectional fluid flow. *Acta Biomaterialia* **2013**; 9: 4673-80. doi:10.1016/j.actbio.2012.08.031
4. Serpooshan V, Quinn TM, Muja N, Nazhat SN. Characterization and modelling of a dense lamella formed during self-compression of fibrillar collagen gels: implications for biomimetic scaffolds. *Soft Matter* 2011; **7**: 2918-26.
5. Kim SH, Lee JH, Hyun H, Ashitate Y, Park G, Robichaud K, et al. Near-Infrared Fluorescence Imaging for Noninvasive Trafficking of Scaffold Degradation. *Sci Rep* 2013; **3**: 749. doi: 10.1038/srep01198.
6. Karfeld-Sulzer LS, Waters EA, Kohlmeir EK, Kissler H, Zhang X, Kaufman DB, et al. Protein polymer MRI contrast agents: Longitudinal analysis of biomaterials in vivo. *Magn Reson Med* 2011; **65**: 220-8. doi: 10.1002/mrm.22587
7. Karfeld-Sulzer LS. *Engineering MRI-detectable protein polymer hydrogels for in vivo biomaterial analysis*. United States: Proquest, Umi Dissertation Publishing; 2011.
8. Lee HS, Hee Kim E, Shao H, Kook Kwak B. Synthesis of SPIO-chitosan microspheres for MRI-detectable embolotherapy. *J Magn Magn Mater* 2005; **293**: 102-5.
9. Wei K, Serpooshan V, Hurtado C, Diez-Cunado M, Zhao M, Maruyama S, et al. Epicardial FSTL1 reconstitution regenerates the

adult mammalian heart. *Nature* **2015**; 525: 479-85. doi: 10.1038/nature15372.
10. Serpooshan V, Zhao M, Metzler SA, Wei K, Shah PB, Wang A, et al. Use of bio-mimetic three-dimensional technology in therapeutics for heart disease. *Bioengineered* 2014; **5**: 193-7.
11. Hosseini F, Panahifar A, Adeli M, Amiri H, Lascialfari A, Orsini F, et al. Synthesis of pseudopolyrotaxanes-coated Superparamagnetic Iron Oxide Nanoparticles as new MRI contrast agent. *Colloids Surf B Biointerfaces* 2013; **103**: 652–657. doi: 10.1016/j.colsurfb.2012.10.035.
12. Hofmann-Amtenbrink M, Hofmann H, Montet X. Superparamagnetic nanoparticles – a tool for early diagnostics. *Swiss Med Wkly* 2010; **140**: w13081. doi: 10.4414/smw.2010.13081.
13. Mahmoudi M, Hosseinkhani H, Hosseinkhani M, Boutry S, Simchi A, Journeay WS, et al. Magnetic Resonance Imaging Tracking of Stem Cells in Vivo Using Iron Oxide Nanoparticles as a Tool for the Advancement of Clinical Regenerative Medicine. *Chem Rev* 2011; **111**: 253-80. doi: 10.1021/cr1001832.
14. Mahmoudi M, Sant S, Wang B, Laurent S, Sen T. Superparamagnetic iron oxide nanoparticles (SPIONs): Development, surface modification and applications in chemotherapy. *Adv Drug Deliv Rev* 2011; **63**: 24-46. doi: 10.1016/j.addr.2010.05.006.
15. Laurent S, Forge D, Port M, Roch A, Robic C, Vander Elst L, et al. Magnetic Iron Oxide Nanoparticles: Synthesis, Stabilization, Vectorization, Physicochemical Characterizations, and Biological Applications. *Chem Rev* 2008; **108**: 2064-10. doi: 10.1021/cr068445e
16. Serpooshan V, Julien M, Nguyen O, Wang H, Li A, Muja N, et al. Reduced hydraulic permeability of three-dimensional collagen scaffolds attenuates gel contraction and promotes the growth and differentiation of mesenchymal stem cells. *Acta Biomater*. 2010; **6**: 3978-87. doi: 10.1016/j.actbio.2010.04.028.
17. Abou Neel EA, Cheema U, Knowles JC, Brown RA, Nazhat SN. Use of multiple unconfined compression for control of collagen gel scaffold density and mechanical properties. *Soft Matter* 2006; **2**: 986-92.
18. Subbiahdoss G, Sharifi S, Grijpma DW, Laurent S, van der Mei HC, Mahmoudi M, et al. Magnetic targeting of surface-modified superparamagnetic iron oxide nanoparticles yields antibacterial efficacy against biofilms of gentamicin-resistant staphylococci. *Acta Biomater.* **2012**; 8: 2047-55. doi: 10.1016/j.actbio.2012.03.002.
19. Taylor EN, Kummer KM, Durmus NG, Leuba K, Tarquinio KM, Webster TJ. Superparamagnetic Iron Oxide Nanoparticles (SPION) for the Treatment of Antibiotic-Resistant Biofilms. *Small Weinh Bergstr Ger* 2012; **8**: 3016-27.
20. Hajipour MJ, Fromm KM, Akbar Ashkarran A, Jimenez de Aberasturi D, Larramendi IRd, Rojo T, et al. Antibacterial properties of nanoparticles. *Trends Biotechnol* **2012**; 30: 499-511. doi: 10.1016/j.tibtech.2012.06.004.
21. Mahmoudi M, Serpooshan V. Silver-coated engineered magnetic nanoparticles are promising for the success in the fight against antibacterial resistance threat. *ACS Nano* **2012**; 6: 2656-64. doi: 10.1021/nn300042m.
22. Xiu ZM, Zhang QB, Puppala HL, Colvin VL, Alvarez PJJ. Negligible particle-specific antibacterial activity of silver nanoparticles. *Nano Lett* **2012**; 12: 4271-5. doi: 10.1021/nl301934w.
23. Kandi V, Kandi S. Antimicrobial properties of nanomolecules: potential candidates as antibiotics in the era of multi-drug resistance. *Epidemiol Health* 2015; 37: e2015020-0. doi: 10.4178/epih/e2015020.
24. Serpooshan V, Mahmoudi M, Zhao M, Wei K, Sivanesan S, Motamedchaboki K, et al. Protein Corona Influences Cell–Biomaterial Interactions in Nanostructured Tissue Engineering Scaffolds. *Adv Funct Mater* **2015**; 25: 4379-89. doi: 10.1002/adfm.201500875